Supporting Information

Precise-Control Synthesis of α-/β-MnO_2 Materials by Adding $Zn(acac)_2$ as a Phase Transformation-Inducting Agent

Ningqiang Zhang[a], Lingcong Li[a], Jinsheng Zhao[c], Tingting Yang[c], Hong He [a,b*], Shaorui Sun[a*]

[a] Key Laboratory of Beijing on Regional Air Pollution Control, Beijing Key Laboratory for Green Catalysis and Separation, Laboratory of Catalysis Chemistry and Nanoscience, Department of Chemistry and Chemical Engineering, College of Environmental and Energy Engineering, Beijing University of Technology, Beijing 100124, China

[b] Shandong Key Laboratory of Chemical Energy Storage and Novel Cell Technology, Liaocheng University, Liaocheng, 252059, China

[c] Collaborative Innovation Center of Electric Vehicles in Beijing, Beijing 100081, China

1. Materials synthesis details

All the chemicals are of analytical grade and used as received without further purification, and deionized water is used throughout. The commercial β-MnO_2 was purchased from Huitong Hunan Science and Technology Co., LTD.

For the synthesis of the α-MnO_2 （HMO）, an aqueous solution (75 mL) containing $MnSO_4 \cdot H_2O$ (2.4840 g) and $KMnO_4$ (1.6590 g) were put into a 100 mL Teflon-lined stainless steel autoclave. Sealed and maintained at 160 °C for 24 h. The resulting black slurry was filtered, washed with deionized water for four times, and then dried at 110 °C for 24 h.[1]

In a typical procedure for the synthesis of mixed-MnO_2, an aqueous solution (75 mL) containing $MnSO_4 \cdot H_2O$ (2.4840 g), $KMnO_4$ (1.6590 g), and desired amounts of $Zn(acac)_2$ (The $Zn(acac)_2$ was weighed using a thermogravmetric microbalance with a precision of 0.0001 mg) were put into a 100 mL Teflon-lined stainless steel autoclave, and then it was sealed, and maintained at 160 °C for 24 h. The resulting black slurries were filtered, washed with deionized water for four times, and then dried at 110 °C for 24 h. All the samples were calcined at 500 °C in air for 6 h before use.

2. Characterization

The crystal structures of the materials were identified by means of X-ray powder diffraction (XRD) over a Bruker D8 Advance X-ray diffractometer with Cu Kα (1.5406 Å) radiation. The data were collected with a scanning speed of 2°/min and a step size of 0.02 ° over the angular range 2θ (10 ° < 2θ < 80°) at 40 kV and 40 mA. The phase compositions of MnO_2 materials with Zn/Mn molar ratio of 0, 0.00050, 0.00175, 0.00200, 0.03850 were investigated by XRD. The data of samples were analysed using the Rietveld refinement technique using HighScore Plus program. The data of the samples were analysed using the Rietveld refinement technique using the HighScore Plus program. The details of the Rietveld refinement steps are as follows: First, the phase structure was determined as follows: “strip *k*-Alpha2, determine background, search peaks, search and match (execute search and match), and chose the pdf code”. Second, Rietveld refinement was carried out as follows: “convert pattern to phase, Rietveld refinement based on the structure”, (1) automatic mode. Is the GOF-index scale below 2.0? If yes, the Rietveld refinement process

completed. If no, continue the second step in the Rietveld refinement. (2) Semi-automatic mode. The steps are as follows: "use available background, zero shift, preferred orientation, scale factor, unit cell, U, V, W, peak shape, B overall, Extinction." Repeat these steps until the GOF-index scale is below 2.0. The quality and reliability of the Rietveld analysis were quantified using the corresponding figures of merit, R_{wp}, the statistically expected least-squares fit, R_{exp}, the profile residual, R_p, and the goodness of fit, GoF-index. A GoF scale below 2.0 means a perfect fitting.[2]

The high angle annular dark field scanning transmission electron microscopy (HAADF-STEM) images and energy dispersive X-ray spectroscopy (EDX) were recorded on a FEI Titan G2 60-300 instrument with accelerating voltages of 300 and 200 kV, respectively. The instrument was equipped with a Cs corrected probe, and super energy-dispersive X-ray spectroscopy (super-EDX) detector featuring a large solid angle (~1 sr) that enables X-ray count rate in excess of 100 kcps.

SEM images were obtained on a Hitachi S4800 field-emission SEM instrument. The MnO_2 samples were immobilized onto silicon wafers and to be dried in a vacuum desiccator for several hours and then treated by gold sputtering.

The Brunauer−Emmett−Teller (BET) specific surface areas and pore volume were determined by nitrogen sorption isotherms on a Micrometritics ASAP 2010 instrument. Samples were pre-degassed at 150 °C for 6 h prior to each measurement to remove physically adsorbed species. The isotherms for adsorption and desorption were measured at relative pressures (P/P_0) from 0.001 to 0.995 and from 0.995 to 0.001, respectively.

Cyclic voltammetry (CV) measurements were conducted on a computer-controlled Autolab potentiostat / galvanostat (PGSTAT302N) in a standard three-electrode electrochemical cell equipped with a gas flow controlling system. The working electrode in the RRDE experiments was a pine model AFE7R9GCPT electrode with a 5.61 mm diameter glassy carbon disk and a Pt ring with an inner diameter of 6.25 mm and an outer diameter of 7.92 mm. A Platinum foil and Ag/AgCl/sat. KCl electrode (0.197 V+0.0591*pH vs. RHE at 25 ^oC) were served as the counter and reference electrode, respectively. For CV measurements, the of 0.1 M phosphate buffer solution (PBS, pH=7.0), was used as the electrolyte solution. N_2 or O_2 was used to purge the solution to achieve oxygen-free or oxygen-saturated electrolyte solutions. The working electrode was well polished with alumina suspension (0.3 mm) and rinsed thoroughly with ethanol and water in an ultrasonic bath to remove any alumina residues to create a mirror finish. Then, 8.5 mL of the MnO_2 suspension was quantitatively transferred using a micropipette onto the electrode. The prepared electrode was dried in air dry for further studies and characterizations. Prior to each measurement, high-purity N_2 or O_2 was bubbled into the electrolytic cell for ca. 30 minutes. The gas was flushed over the solution during the measurements.

3. Figures

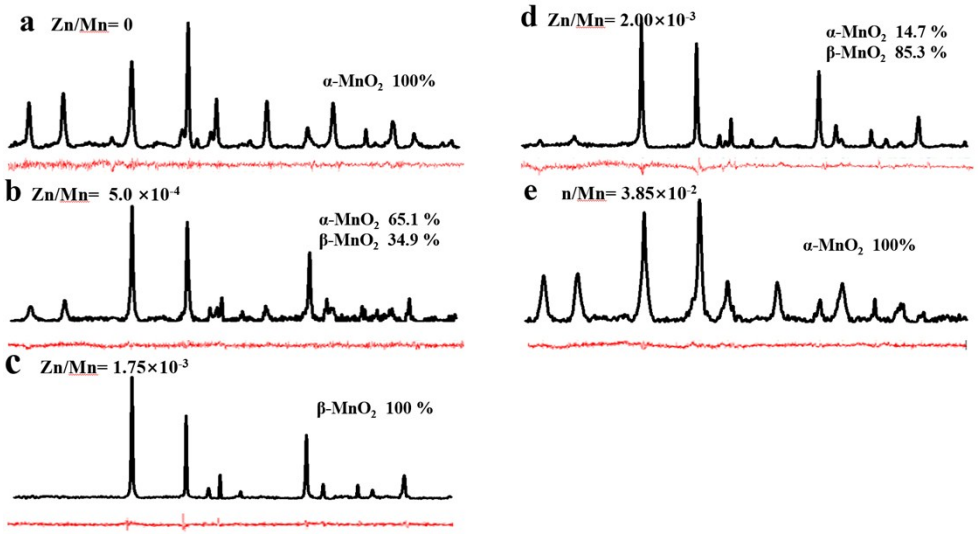

Figure S1. Rietveld refinement for the MnO_2 materials (the red lines represent the different plot of the rietveld result)

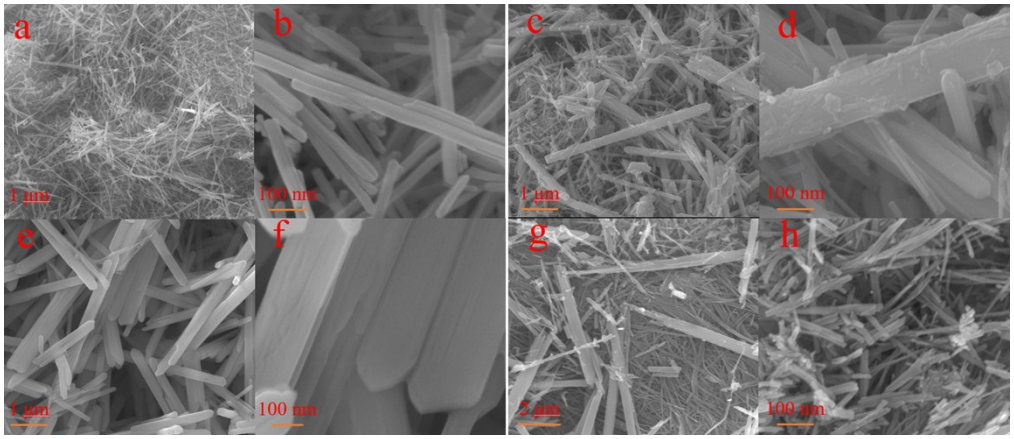

Figure S2. SEM images of mix-phase MnO_2 materials with the Zn/Mn ratios of 0 (a, b), 5.00×10^{-4} (c, d), 1.75×10^{-3} (e, f), 2.00×10^{-3} (g), and 3.85×10^{-2} (h).

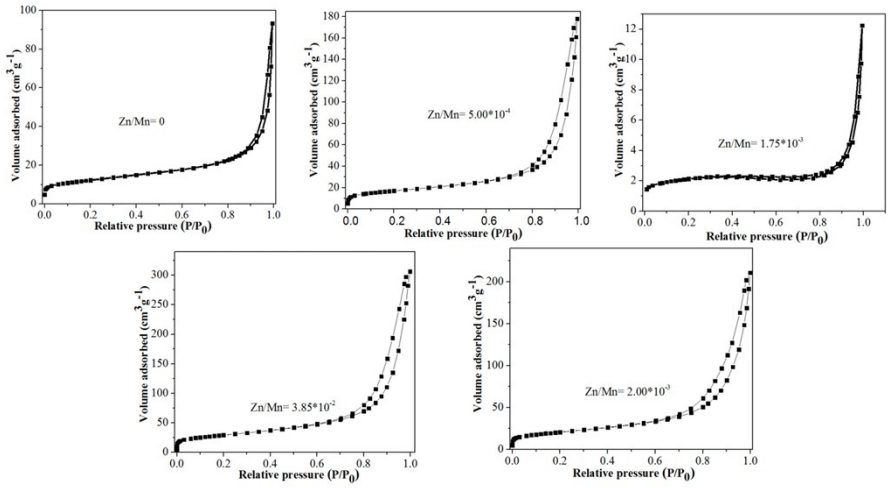

Figure S3. Nitrogen adsorption–desorption isotherms of the MnO_2 samples.

Furthermore, the nitrogen adsorption–desorption isotherms of the MnO_2 materials were measured and the results are shown in Fig. S3. The characteristics type IV hysteresis loop appeared at the P/P_0 range of 0.8-1.0. Interestingly, the BET data in Table S1 and Fig. S3 show that the specific surface area gradually increased with the increase in the amount of $Zn(acac)_2$. However, the specific surface area of β–MnO_2 was 8 m^2/g at the Zn/Mn ratio of 1.75×10^{-3}. This can be attributed to its smallest tunnel size (2.3 Å × 2.3 Å) because of the densely packed manganese octahedral. The introduction of Zn species into the reaction system, promoted the generation of β–MnO_2, providing a large space for anchoring α-MnO_2 nanowires, reducing the denseness of packed manganese octahedral and increasing the degree of disorder of α-MnO_2. Therefore, the BET gradually increased with an increase in the amount of $Zn(acac)_2$ except β–MnO_2.

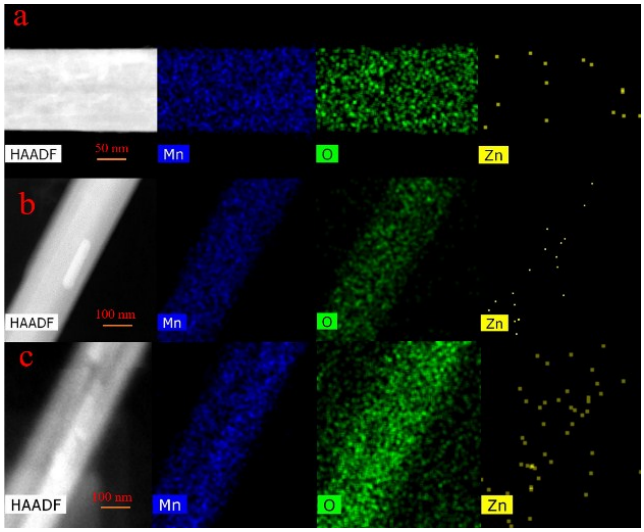

Figure S4. Elemental mapping images of β-MnO_2 in mixed-MnO_2 with the Zn/Mn ratios of 5.0×10^{-4} (a), 1.75×10^{-3} (b), Zn/Mn =2.00×10^{-3} (c).

Furthermore, the dispersion of Zn present in MnO_2 mixture on β-MnO_2 was also investigated using the elemental mapping method, and the results are shown in Figs. S4. The Zn atoms showed a good dispersion along the β-MnO_2 growth direction (0001) at the Zn/Mn ratio of the range of 0 to 1.75×10^{-3}. However, Fig.

S4c shows that when the Zn/Mn ratio was more than 2.00×10^{-3}, the Zn atom spread randomly on the surface of β-MnO_2, and some Zn species were separately located on the β-MnO_2 nanorods. However, all the Zn species still showed a good dispersion.

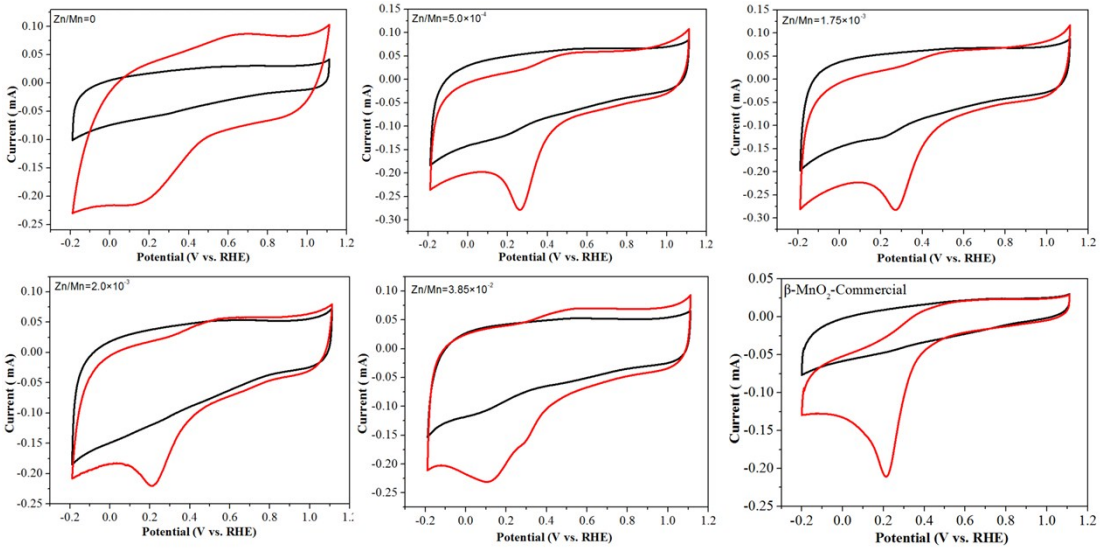

Figure S5. CV curves of different MnO_2 under N_2-saturated (black line) and O_2-saturated (red line). 0.1 M PBS aqueous solutions at a scan rate of 100 mVS^{-1} between -0.2 and 1.1 V.

4. Tables

Table S1. BET Surface Area, Pore Volume, and Chemical Composition (EDX)

Mix-MnO_2 sample (Zn/Mn atom ratio)	Pore Volume (cm^3/g)	BET Surface Area (m^2/g)	Zn/Mn ratio by EDX
0	0.137	40	0
5.00×10^{-4}	0.257	58	6.02×10^{-4}
1.75×10^{-3}	0.017	8	2.01×10^{-3}
2.00×10^{-3}	0.290	71	2.12×10^{-3}
3.85×10^{-2}	0.430	102	2.97×10^{-2}

Table S2. Rietveld refined XRD parameters of Mixed-MnO_2 materials

sample (Zn/Mn atom ratio)		0	5.00×10^{-4}	1.75×10^{-3}	2.00×10^{-3}	3.85×10^{-2}
Phase contents						
	α	100%	34.9%	0	14.7%	100%
	β	0	65.1%	100%	85.3%	0
Space group						
	α	I4/m (87)	I4/m (87)		I4/m (87)	I4/m (87)
	β		P42/mnm (136)	P42/mnm (136)	P42/mnm (136)	
Cell parameters						
α	a (Å)	9.7847	9.8075		9.8283	9.8150
	c (Å)	2.8630	2.8645		2.8607	2.8470
β	a (Å)		4.4071	4.4035	4.4050	
	c (Å)		2.8740	2.8741	2.8744	
R-factors						
	R_{exp} (%)	5.20	4.64	2.90	5.81	2.07
	R_p (%)	3.50	3.32	2.31	5.85	1.77
	R_{wp} (%)	4.57	4.18	3.00	7.51	2.23
	GOF-index	0.88	0.81	1.07	1.67	1.07

Table S3. Summary of the ORR Catalytic Performance Revealed from CV curves

Mix-MnO_2 sample (Zn/Mn atom ratio)	Oxygen reduction potential (V)	Oxygen reduction currents (mA)
0	0.16	-0.21
5.0×10^{-4}	0.26	-0.21
1.75×10^{-3}	0.27	-0.28
2.00×10^{-3}	0.22	-0.22
3.85×10^{-2}	0.12	-0.23
β-MnO_2-Commercial	0.21	-0.21

1. Z. Huang, X. Gu, Q. Cao, P. Hu, J. Hao, J. Li and X. Tang, *Angewandte Chemie*, 2012, **51**, 4198-4203.
2. T. Degen, M. Sadki, E. Bron and U. K. G. Nénert, *Powder Diffraction*, 2014, **29**, S13-S18.